Int. J. Electrochem. Sci., 14 **(2019)** 7717 – 7728, doi: 10.20964/2019.08.01

International Journal of
ELECTROCHEMICAL
SCIENCE
www.electrochemsci.org

Properties of Jet electrodeposition Nickel Coating on TC4 Alloy Prepared by Selective Laser Melting

Xiao Wang[1], *Zhanwen Wang*[1], *Lida Shen*[*], *Mingyang Xu, Kai Wang, Zongjun Tian*

National Key Laboratory of Science and Technology on Helicopter Transmission,
Nanjing University of Aeronautics and Astronautics, Yu Dao Street, 210016 Nanjing, China
[1]These authors contributed equally to this work
[*]E-mail: ldshen@nuaa.edu.cn

Received: 21 January 2019 / *Accepted:* 18 March 2019 / *Published:* 30 June 2019

In order to solve the problems of poor surface wear resistance and low hardness of titanium alloy materials formed by selective laser melting (SLM) technology, a new method of preparing bright nickel protective coating by jet electrodeposition was proposed in this paper. The surface morphology of the coatings was characterized by field emission scanning electron microscopy. The microhardness tester, scratch tester, and friction and wear tester were used to analyze the adhesion, hardness, and wear resistance of the coatings. The results indicated that the current density has an important effect on the properties of the coatings; as the current density increases, the surface flatness gradually increases and then decreases. When the current density is 120 A/dm^2, the microhardness of the coatings reaches 548 HV, and the adhesion strength also reaches 30.4 N. Compared with the surface of titanium alloy, the surface of the coating has better wear resistance, and the surface is more complete after friction and wear test. The wear mechanism is transformed from microscopic grinding to smearing.

Keywords: SLM; jet electrodeposition; adhesion strength; wear resistance

1. INTRODUCTION

Titanium and titanium alloys have been widely used in modern industry because of their low density, high specific strength, superior high temperature mechanical properties, low temperature resistance, good brittleness, and heat resistance [1-5]. In recent years, the development of titanium and titanium alloys has been very rapid, especially in the aviation industry, where the demand for titanium alloys has grown more quickly [6-7]. Manufacturing technology for powder metal adding material based on layer by layer accumulating forming idea, such as SLM, provides a new idea for the integrated design and manufacture of complex titanium alloy structures. Its basic principle is to melt metal powder layer by layer according to the pre-planned scanning path by using high energy beam

energy source, directly forming the parts. This technology is suitable for many fields [8]. Many scholars have carried out extensive studies and achieved numerous results [9-10]. However, titanium alloys formed by SLM technology have poor wear resistance, are prone to contact corrosion, and have poor electrical and thermal conductivity, seriously restricting their application [11-12]. Therefore, it is necessary to apply some surface treatments on the titanium alloy in order to expand its application scope and improve its service life.

The surface treatment methods of titanium alloys include anodic oxidation [13], micro-arc oxidation [14], electroplating [4, 15], and electroless plating [16]. Among them, the method of anodic oxidation and micro-arc oxidation forms a dense oxide film on the surface of the titanium alloy, protecting the titanium alloy. However, because of its thin film and poor wear resistance, its performance is seriously affected. Electroplating deposits a coating on the surface of the titanium alloy by the principle of cathode deposition, which has the characteristics of uniformity and low porosity. Therefore, the properties of titanium and its alloys can be improved by deposition protection. [17-21]. There have been many scholars who have previously explored this area. Xia et al. show that NiCrAlY coating can significantly improve the ablation resistance of TC6 titanium alloy [17]. Peng et al. found that the deposition of Ta-W coating has a very good effect on protecting titanium and its alloys in an ablation atmosphere [22]. Yu et al. obtained a copper plating layer with good adhesion strength by activating and hydrogenating the titanium alloy. It was found that the electroplated copper improved the conductivity of the titanium alloy matrix and weakened its galvanic corrosion tendency [23].

Owing to the flexibility, being able to adapt to different surfaces, and having a large limiting current density of jet electrodeposition, we attempt to deposit a nickel coating on the titanium alloy formed by SLM using jet electrodeposition. In this paper, we will research the effects of different current densities on the surface morphology, adhesion, hardness, and wear resistance of the coatings.

2. EXPERIMENTAL

2.1 Experimental device

The CNC jet electrodeposition system used in this experiment is built independently. The main part of the system consists of transmission system, solution circulation system, and control system, which can control the jet moving range, scanning speed, and deposition time. The auxiliary part ensures the stability of solution temperature during electrodeposition. The physical equipment is shown in Fig. 1. The X-axis motor controls the anode to reciprocate, the Z-axis motor controls the anode to move up and down, and the nozzle and work-piece stage are printed by fused deposition modeling (FDM). During processing, the self-priming pump sucks the solution from the plating bath into the anode chamber, followed by spraying the solution to the surface of the cathode work-piece through the nozzle, and finally starting to deposit after electrification.

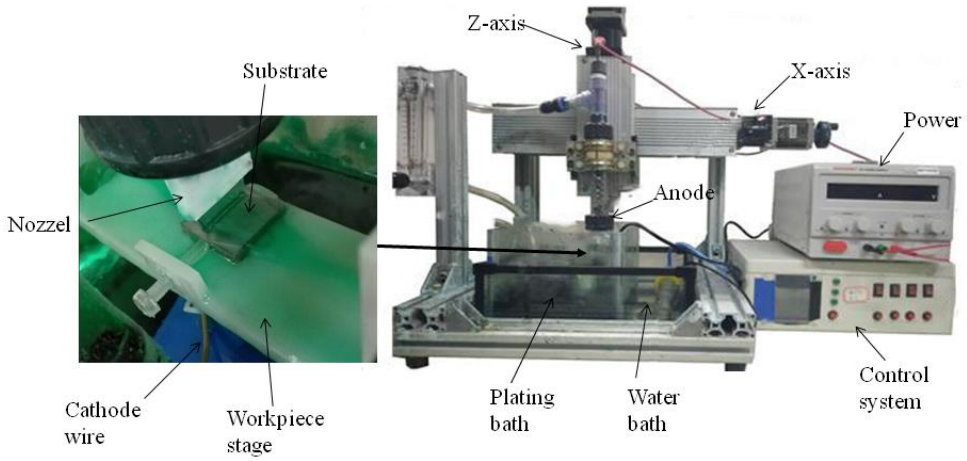

Figure 1. Experimental device

2.2 Experimental process and parameters

Titanium alloy formed by SLM technology was selected as the experimental substrate. Its size was15×15×3 mm, in which the laser scanning rate was 840 mm/s, the power was 220 W, and TC4 powder was used with an average particle size of 30 μm. The surface of titanium alloy was manually polished with 400#, 800#, 1000# metallographic sandpaper, followed by ultrasonic cleaning with deionized water, and alcohol, membrane removal, ultrasonic cleaning with deionized water, and nickel plating.

Table 1. Electroplating bath composition and processing parameters

	Composition and operating conditions	Content
Solution	$NiSO_4 \cdot 6H_2O$ (g/L)	280
	$NiCl_2 \cdot 6H_2O$ (g/L)	40
	H_3BO_4 (g/L)	40
	$C_7H_5O_3NS$ (g/L)	5.0
	PH	4.0±0.1
Operating conditions	Nozzle size(mm)	20×1
	Anode-cathode distance(mm)	2.0
	Rate of flow (L/h)	200
	Scanning speed (mm/s)	5
	Temperature (°C)	50±1.0

The composition and processing parameters of the plating solution are shown in Table 1. The reagents in all of the solutions are analytically pure. The role of $NiSO_4 \cdot 6H_2O$ and $NiCl_2 \cdot 6H_2O$ in the solution is to provide nickel ions for the deposition process, and the role of $C_7H_5O_3NS$ is to refine the grains [24]. The addition of H_3BO_4 not only adjusts the pH of the solution, but also enhances the electrolyte polarization layer [25]. The parameters of current and deposition time are shown in Table 2.

Table 2. Samples with different process parameters

Sample number	Working current(A/dm^2)	Plating time (min)
1	60	40
2	80	30
3	100	24
4	120	20
5	140	17

2.3 Properties characterization

Table 3 shows the test equipment for analyzing the surface morphology, microhardness and protective properties of coatings, as well as their models and parameters.

Table 3. Testing equipment

Instruments (Type)	Parameters	Characterization
Scanning electron microscopy (S-4800)	5.0kV ×500 or 5.0kV ×50 or 5.0kV ×2000	Surface morphology
Micro-hardness tester (HXS-1000A)	Load 2N, loading time 10s	Micro-hardness
Scratch tester (WS-2005)	40N, 3mm,Friction force	Adhesion strength
Friction and wear (HSR-2M)	Load 10N, loading time 240s	Wear resistance

3. RESULTS AND DISCUSSION

3.1 Surface morphologies

The surface micro-morphology of pure nickel coatings prepared at different current densities is shown in Fig. 2. From the figure, it can be observed that there are different cell sizes and micro-bumps on the surface of the coatings. This is attributable to the fact that the surface of titanium alloy is only polished by hand with sandpaper. It is unavoidable that there are a lot of micro-protrusions on the surface of titanium alloy. At the same time, preferentially generated nuclei will also increase the surface roughness of the cathode. Affected by the "edge effect", the electric field strength of the bulge is higher than that of the concave area, causing the deposition speed of each part of the titanium alloy surface to be different. When the current density is 80 A/dm^2, as shown in Fig. 2a, both the deposition velocity difference of different parts and the nucleation point on the cathode surface are small because of the small current, resulting in a small number of crystal cells on the cathode surface. In addition, the low current causes less nickel to be deposited on the substrate per unit time, and the liquid flow rate is higher, which has a certain scouring effect on the cathode surface. To a certain extent, it will destroy

the surface of the deposited layer and make the surface have a small amount of ravine stripes [26]. When the current density increases to 100 A/dm^2, a slightly uneven position on the surface of the titanium alloy will quickly form a bulge because of the high current density, and as the deposition proceeds, the bulge will become increasingly more obvious. Compared with Fig. 2a, the number of cellular bumps on the surface of the coating noticeably increases, as shown in Fig. 2b. This is attributable to the increase of nucleation points on the cathode surface caused by the high current. As the current density continues to increase to 120 A/dm^2, the nucleation points on the surface of the substrate continue to grow in number. Further, the curvature of the cellular processes is larger, the equipotential lines are denser, and the electric field intensity significantly increases. Owing to the electric field being shielded by large protrusions, many small protrusions gradually stop growing during continuous deposition, and the growth rate of large protrusions becomes faster and faster, making them collide with each other and submerge small protrusions. The large protrusions that collide with each other improve the smoothness of the coating to a certain extent. As shown in Fig. 2c, the morphology of the coating is obviously better that observed in Fig. 2a and Fig. 2b. As shown in Fig. 2d, when the current density is increased to 140 A/dm^2, the surface of the plating layer has defects such as large protrusions and pits. On the one hand, this is caused by the current density being too high and the deposition rate being too fast. On the other hand, nickel ions in the vicinity of the cathode are rapidly consumed, and a serious shortage of nickel ions causes hydrogen ions in the solution to be reduced, thereby increasing plating defects [27].

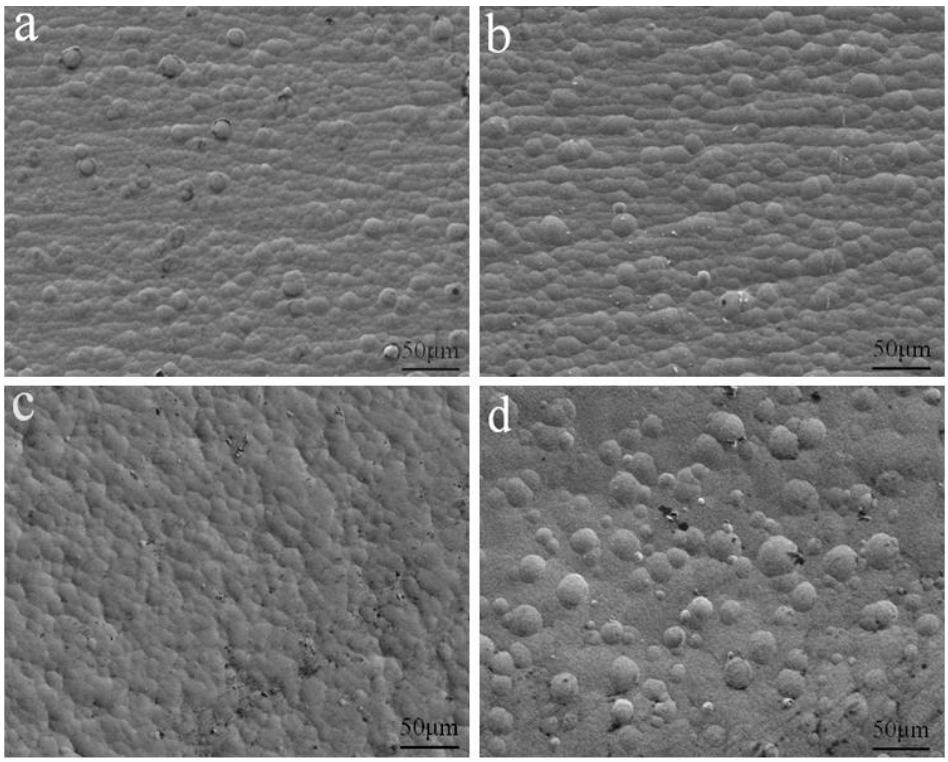

Figure 2. Surface morphology of coatings (a.80A/dm^2;b.100A/dm^2;c.120A/dm^2;d.140A/dm^2)

3.2 Adhesion strength

The cross-section morphology and scratches of the samples are shown in Fig. 3. The samples are cut by a wire-cutting machine, then gently polished and washed with alcohol. Fig. 3a depicts cross-section morphology with current density of 60 A/dm^2. It can clearly be seen that there is a slight gap between the coating and the substrate, adhesion effect is not ideal. Fig. 3c presents the cross-section morphology of 120 A/dm^2 current density. In the figure, the coating and the substrate adhesion are very close without any obvious cracks, and even some Ni are embedded in the substrate. It can be inferred that the coating with current density of 120 A/dm^2 has stronger adhesion strength than that with current density of 60 A/dm^2.

In this test, the scratch method was used to quantitatively analyze the bonding force between the coating and substrate. When the frictional force significantly fluctuates, this denotes that peeling occurs between the coating and the substrate, and the value of the load applied at this time is used as a basis for evaluation. Fig. 3b and Fig. 3d show the indentation of current density of 60 A/dm^2 and 120 A/dm^2, respectively. It can be seen that the indentation of Fig. 3b is obviously fractured and falls off. The indentation of Fig. 3d has no cracks until the end, which is consistent with the results of cross-section morphology of Ni coatings on substrate. The adhesion strength of the coating is shown in Fig. 4. When the current density increases, the adhesion of the coatings first increases. When the current density is 120 A/dm^2, the adhesion strength of the coatings reaches the maximum of 30.4 N, and then decreases with the increase of the current density.

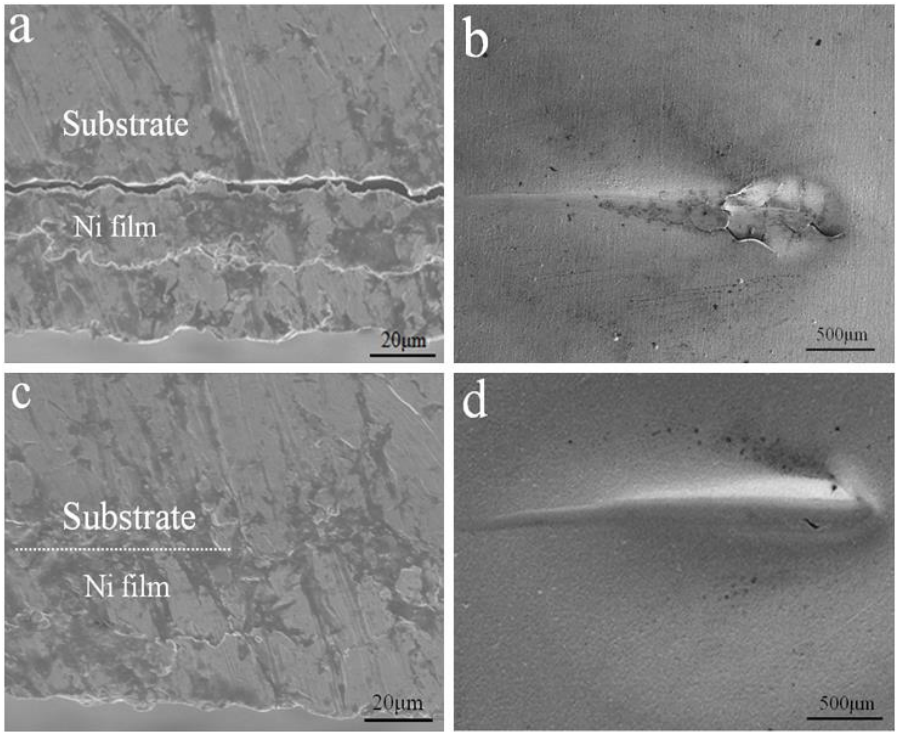

Figure 3. Cross-section morphology of Ni coatings on substrate and surface morphology after scratch test (a, b.60A/dm^2; c, d.120A/dm^2)

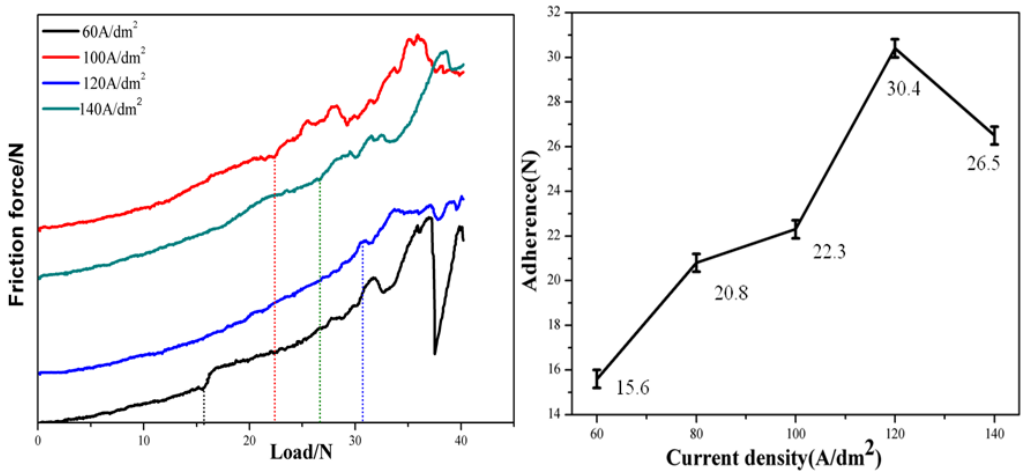

Figure 4. Coating adhesion strength prepared at different current densities

Since the surface of titanium alloy is only polished by hand, there are inevitably protrusions and depressions, as well as gully-like stripes, on the surface. When the current density is low, the surface of the coating has fewer nucleation points. Further, because of the "edge effect", nickel ions will preferentially deposit on the protruding part of the substrate surface. The pitting and gully-like stripes on the substrate surface cause a slight gap between the coating and the substrate, seriously affecting the adhesion strength between the substrate and the coating. However, when the current density is increased, the surface nucleation point is increased, the plating defects are reduced, the uniformity and density of the plating layer are improved, and the adhesion strength is greatly improved. When the current density is too large, the hydrogen evolution reaction will increase because of the lack of nickel ions, and the gas and impurities generated by the reaction will remain between the substrate and the coating, easily causing cracking of the coating and reducing the adhesion strength.

3.3 Microhardness.

Fig. 5 shows the microhardness of the nickel coatings prepared at different current densities on titanium alloy. The microhardness of nickel coating first increases and then decreases with the increase of current density. The maximum microhardness is 548 HV, and the corresponding current density is 120 A/dm^2. Then, with the increase of current density, the microhardness of the coating gradually decreases. The dashed line in the figure shows the hardness of the titanium alloy formed by SLM technology, which is 372.1 HV. It can be seen that its hardness is low. One reason for this is that some of the powder particles in the SLM process are not fully melted, resulting in voids [28]. Second, the stability of laser energy output and the error of powder layer thickness make the forming quality of each layer slightly different, thus affecting the overall hardness of titanium alloy [29].

The surface microhardness of the coating is not only affected by the grain size of the coating [30], but also by the density, purity, number of defects and structure of the coating [25, 31]. In general, the coating defects are reduced, the surface quality is better, and the coating hardness is higher. From the above analysis of the surface morphology of the coatings, it can be observed that the surface

morphologies of the coatings prepared with different current densities are different. When the current density is 120 A/dm^2, the surface defects of the coating are few, and the density is high, so its hardness reaches the maximum. Continuous increase of current density will increase the number of surface defects and larger cellular processes, significantly affecting the microhardness of the coatings.

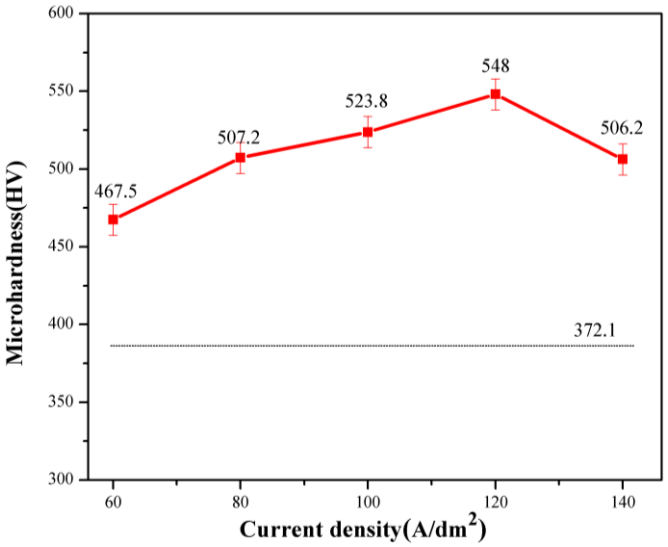

Figure 5. Microhardness of the coating under different current density

3.4 Wear resistance

Fig. 6 shows the surface morphology of different samples after wear test. Fig. 6a is the morphology of titanium alloy after wear test. It can be observed from the figure that the surface is almost entirely all deep furrows. It can be considered that the wear mechanism is mainly microscopic grinding, indicating that the surface hardness of pure titanium is low and the wear resistance is poor. According to the hardness analysis above, the hardness of titanium alloy formed by SLM technology is not high and the strength is low. Most materials are easy to fall off under the action of micro-cutting and form abrasive debris, which attaches to the friction surface. This, further aggravates the wear, and makes the volume of wear increase, thus forming a deep plough-groove-like wear mark on the surface; Fig. 6b is its partial enlargement morphology. Fig. 6c is the surface of the coating with current density of 60 A/dm^2. From the morphology of the coatings after wear, there are obvious cracks, peeling, and shedding, indicating that the plastic deformation of the coatings has taken place. It is more obvious from its local enlarged morphology (Fig. 6d), indicating that the wear resistance of the coatings with current density of 60 A/dm^2 is poor. Fig. 6e is the wear surface of nickel coating with current density of 120 A/dm^2. From the morphology, it can be understood that the coating is relatively complete on the whole, the wear grooves are sparse and shallow, and there are wear marks parallel to the direction of motion on the surface of the coating. It can be considered that the wear mechanism of the coating is mainly smearing, showing that the wear resistance of the coating is better [32]. This is also the best wear resistance of the five sets of different current densities samples. The reason for this phenomenon is that when the current density is low, there are fewer nucleation points on the cathode surface and the

nucleation speed of the grains is slow, resulting in the lower compactness, coverage, adhesion, and hardness of the coating, and worsening the wear resistance. When the current density is high, the deposition rate of cathode surface is too fast, and defects such as nodulation, pitting, and burning are easily formed on the coating surface [33]. These factors are not conducive to improving the wear resistance of the coating surface. Therefore, when the current density is 120 A/dm^2, the wear resistance is the best.

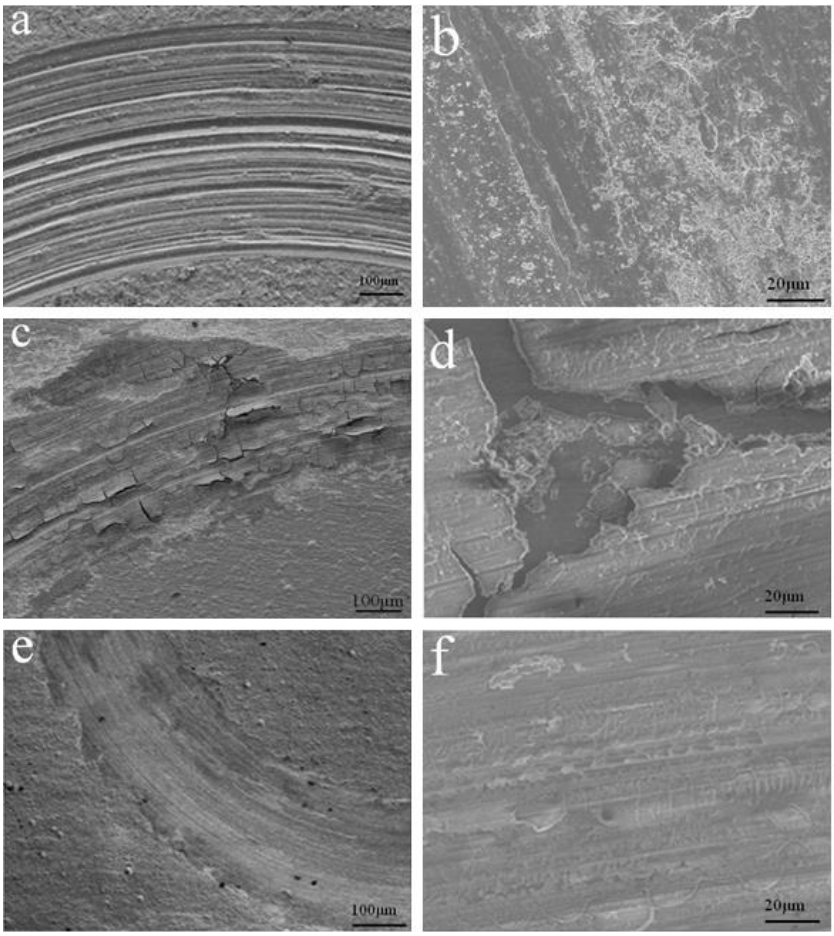

Figure 6. Surface morphology after coating wear (a, b. titanium alloy surface; c, d. 60 A/dm^2; e, f. 120 A/dm^2)

In order to further verify the above viewpoint, the variation of surface friction coefficient of nickel coatings with different current densities is studied. As shown in Fig. 7, the friction coefficient of the sample is relatively small at the initial stage of wear, and then rapidly increases. This is attributable to the friction between the coating, and the grinding ball mainly occurs in the uneven area of the coating. At this time, the contact area between the coating and the grinding ball is small, leading to the reduction of friction resistance, and causing the friction coefficient of the coating to be low at first. As the friction continues, the contact area gradually increases, and the adhesion between the grinding head and the coating is strengthened because of the heat generation of friction. This results in a rapid

increase in friction coefficient, and finally stabilizing in a stable region, i.e., the stable wear stage [34]. The friction coefficient of the coating with different current densities has a certain fluctuation. From Figure 7, the friction coefficient of the sample with current density 120 A/dm^2 is the smallest, about 0.65-0.7, followed by 140 A/dm^2 and 60 A/dm^2, about 0.8-0.85. When the experimental conditions are fixed, the surface of the coating has more rough peaks when the friction coefficient is large, while the surface roughness peaks are less when the friction coefficient is small [35].

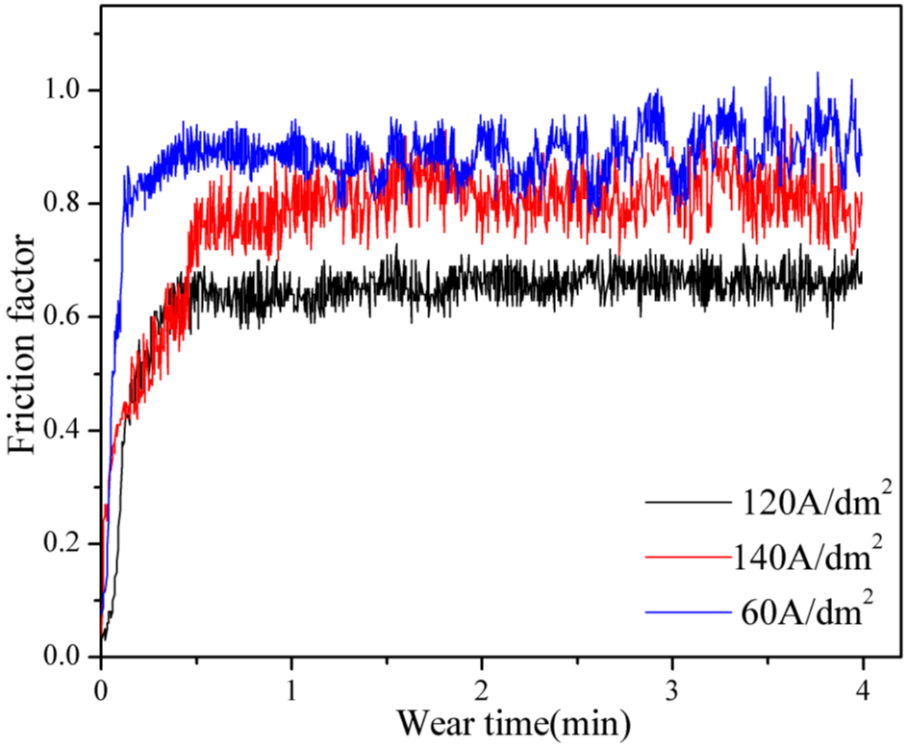

Figure 7. Relationship between friction coefficient of coatings and time

4. CONCLUSIONS

(1) Smooth and compact nickel coating can be deposited on the surface of TC4 formed by SLM technology by using appropriate current density (120 A/dm^2). When the current density is too low or too high, there will be many bumps or defects on the surface of the nickel coating.

(2) With the increase of current density, the adhesion and hardness of the coating increases first and then decreases. When the current density is 120 A/dm^2, the coating adhesion reaches the highest at 30.4 N, and the microhardness increases from 372 HV on TC4 surface to 548 HV.

(3) The wear mechanism of pure titanium substrate is microscopic grinding, with deep furrows on the surface. When the current density increases from 60 A/dm^2 to 120 A/dm^2, the wear mechanism of nickel coating changes from fatigue wear to smearing, with the friction coefficient obviously decreasing. It is indicated that nickel plating on the titanium alloy can effectively improve its overall wear resistance.

ACKNOWLEDGMENTS
The project is supported by the National Natural Science Foundation of China (Grant No. 51475235, No. 51105204 and No.U1537105). We also extend our sincere thanks to all who contributed in the preparation of these instructions.

References

1. M. Long and H.J. Rack, *wear*, 249(2001)157.
2. T. Zhao, X. Lu and X. Qu, *Technology*, 30(2012)300.
3. O. Prymak, D. Bogdanski, M. Koller, G. Muhr, F. Beckmann, T. Donath, M. Assad and M. Epple, *Biomaterials*, 26 (2005) 5801.
4. Z.H. Sun, Y.H. Liu, X.Y. Zhang, Z.H. Tang and M.H. Liu, *corrosion & protection*, 26 (2005) 493.
5. H.J. Rack and J.I. Qazi, *Materials Science and Engineering C*, 26 (2006) 1269.
6. S.L. Semiatin, D.M. Dimiduk, K.H.G. Ashbee and V. Seetharaman, *Metallurgical and Materials Transactions A*, 29(1998)7.
7. Z.S. Zhu, *Journal of Aeronautical Materials*, 34 (2014)44.
8. D.D. Gu, Q.M. Shi, K.J. Lin and L.X. Xi, *Additive Manufacturing*, 22 (2018) 265.
9. L.E. Murr, S.M. Gaytan, A. Ceylan, E. Martinez, J.L. Martinez, D.H. Hernandez, B.I. Machado, D.A. Ramirez, F. Medina, S. Collins and R.B. Wicker, *Acta Mater.*,58 (2010) 1887.
10. B. Baufeld, B.O. vander and R. Gault, *Mater. Des.*, 31 (2010) 106.
11. Z.S. Zhu, X.N. Wang, L. Tong and G.Q. Shang, *Materials China*, 5(2010)14.
12. Q. Ru, X.Q. Hu and G. Sheng, *Guangdong Chemical Industry*, 4(2010)18.
13. X.L. Wu, Y.T. Li and C.Y. Xie, *Science and Technology*, 1(2009)15.
14. H. Zhou, Z.T. Liu, Z.X. Li and J.H. Du, *Rare Metal Mat. Eng.*, 34 (2005)1835.
15. W.Y. Zhou and S.W. Kang, *Materials Protection*, 39(2006)72.
16. E.J. Tang, Z. Liu and Y.Q. Zhao, *Electroplating & Pollution Control*, 23 (2003)21.
17. X.M. Peng, C.Q. Xia, X.Y. Dai, A.R. Wu, L.J. Dong, D.F. Li and Y.R. Tao, *Surf. Coat. Technol.*, 232 (2013) 690.
18. X.M. Peng, C.Q. Xia, X.Y. Dai, A.R. Wu, L.J. Dong, D.F. Li and Y.R. Tao, *Surf. Coat. Technol.*, 232 (2013) 254.
19. C. Leyens, J.V. Liere, M. Peters and W.A. Kaysser, *Surf. Coat. Technol.*, 108 (1998) 30.
20. X.M. Yu, L.L. Tan, H.Z. Yang and K. Yang, *J. Alloy. Compd.*, 644 (2015) 698.
21. D.B. Wei, P.Z. Zhang, Z.J. Yao, J.T. Zhou, X.F. Wei and P. Zhou, *Appl. Surf. Sci.*, 261 (2012) 800.
22. X.M. Peng, C.Q. Xia, L. Zhou, L. Huang, D.F. Li and A.R. Wu, *Surf. Coat. Technol.*, 349 (2018) 622.
23. H. Yu, Y.F. Li, Z.Y. Wang, C. Cao and J. Gao, *Corrosion and Protection*, 36 (2015)432.
24. Y.H. Wang, L.D. Shen, M.B. Qiu, Z.J. Tian, X. Liu and W. Zhuo, *J. Electrochem. Soc.*, 163 (2016) 579.
25. W. Zhu, L.D. Shen, M.B. Qiu, Z.J. Tian and W. Jiang, *Surf. Coat. Technol.*, 333 (2018) 87.
26. S.J. Ma, L.D. Shen, Z.J. Tian, Z.D. Liu, Y.H. Huang and G.F. Wang, *materials for mechanical engineering*, 36(2012)17.
27. L.D. Shen, Y.H. Wang, W. Jiang, X. Liu, C. Wang and Z.J. Tian, *Corros. Eng. Sci. Technol.*, 52(2017)311.
28. Y.L. Xu, D.Y. Zhang, X.Y. Cao and Y. Zhou, *Applied Laser*, 37(2017)199.
29. J.P. Kruth, L. Froyen, J.V. Vaerenbergh, P. Mercelis, M. Rombouts and B. Lauwers, *J. Mater. Process. Technol.*, 149 (2004) 616.
30. K.L. Zhao, L.D. Shen, M.B. Qiu, Z.J. Tian and W. Jiang, I*nt. J. Electrochem. Sci.*, 12 (2017) 8578.
31. L.D. Shen, W. Zhuo, M.B. Qiu, Z.J. Tian and C. Wang, *Int. J. Electrochem. Sci.*, 12 (2017) 9040.

32. I. Garcia, J. Fransaer and J.P. Celis, *Surf. Coat.Technol.*, 148 (2001)171.
33. G.F. Wang, L.D. Shen, L.M. Dou, Z.J. Tian and Z.D. Liu, *Int. J. Electrochem. Sci.*, 9 (2014) 220.
34. Z.W. Huang, L. Wang, L. Wang and Y.D. Li, *Diamond & Abrasivers Engineering*, 34(2014)40.
35. G.B. Li, D.L. Guan and T.J. Li, *Journal of Dalian Maritime University,* 35(2009)90.